HHS Public Access

Author manuscript

Heart Vessels. Author manuscript; available in PMC 2018 May 01.

Published in final edited form as:

Heart Vessels. 2017 May ; 32(5): 628–636. doi:10.1007/s00380-017-0955-x.

Conditional knockout of activin like kinase-1 (ALK-1) leads to heart failure without maladaptive remodeling

Kevin J. Morine, **Vikram Paruchuri**, **Xiaoying Qiao**, **Mark J. Aronovitz**, **Emily E. Mackey**, **Lyanne Buiten**, **Jonathan Levine**, **Keshan Ughreja**, **Prerna Nepali**, **Robert M. Blanton**, **Richard H. Karas**, and **Navin K. Kapur**

Molecular Cardiology Research Institute and Division of Cardiology, Department of Medicine, Tufts Medical Center, 800 Washington Street, Boston, Massachusetts, 02111, USA

Abstract

Activin like kinase-1 (ALK-1) mediates signaling via the transforming growth factor beta (TGFβ) family of ligands. ALK-1 activity promotes endothelial proliferation and migration. Reduced ALK-1 activity is associated with arteriovenous malformations. No studies have examined the effect of global ALK-1 deletion on indices of cardiac remodeling. We hypothesized that reduced levels of ALK-1 promote maladaptive cardiac remodeling.

Methods—We studied ALK-1 conditional knockout mice (cKO) harboring the ROSA26-CreER knock-in allele whereby a single dose of intraperitoneal tamoxifen triggered ubiquitous Cre-recombinase mediated excision of floxed ALK-1 alleles. Tamoxifen treated wild-type (WT-TAM; n=5) and vehicle treated ALK-1-cKO mice (cKO-CON; n=5) served as controls for tamoxifen treated ALK-1-cKO mice (cKO-TAM; n=15).

Results—ALK-1 cKO-TAM mice demonstrated reduced 14-day survival compared to cKO-CON controls (13% vs 100%, respectively, $p<0.01$). Seven days after treatment, cKO-TAM mice began to exhibit reduced left ventricular (LV) fractional shortening, progressive LV dilation, and gastrointestinal bleeding. After 14 days total body mass was reduced, but LV and lung mass increased in cKO-TAM not cKO-CON mice. Peak LV systolic pressure, contractility, and arterial elastance were reduced, but LV end-diastolic pressure and stroke volume were increased in cKO-TAM, not cKO-CON mice. LV ALK-1 mRNA levels were reduced in cKO-TAM, not cKO-CON mice. LV levels of other TGFβ-family ligands and receptors (ALK5, TBRII, BMPRII, Endoglin, BMP7, BMP9, and TGFβ1) were unchanged between groups. Cardiomyocyte area and LV levels of BNP were increased in cKO-TAM mice, but LV levels of β-MHC and SERCA were unchanged. No increase in markers of cardiac fibrosis, Type I collagen, CTGF, or PAI-1, were observed between groups. No differences were observed for any variable studied between cKO-CON and WT-TAM mice.

Correspondence to: Navin K. Kapur, MD, Tufts Medical Center, 800 Washington Street, Box # 80, Boston, MA 02111, Telephone: 617-636-9371, Fax: 617-636-1444, Nkapur@tuftsmedicalcenter.org.

Ethical Approval

All applicable international, national, and/or institutional guidelines for the care and use of animals were followed.

Conflict of Interest

The authors declare they have no conflict of interest.

Conclusion—Global deletion of ALK-1 is associated with the development of high output heart failure without maladaptive remodeling. Future studies exploring the functional role of ALK-1 in cardiac remodeling independent of systemic AVMs are required.

Keywords

Activin like kinase 1; Hereditary hemorrhagic telangiectasia; High output heart failure

Introduction

Hereditary hemorrhagic telangiectasia (HHT) is an inherited disorder of vascular homeostasis due to mutations in the genes encoding members of the transforming growth factor beta (TGF-β) signaling pathway including endoglin, activin receptor-like kinase 1 (ALK-1) and SMAD-4 [1]. HHT type 2 is caused by reduced ALK-1 activity and is characterized by systemic small and large vessel arteriovenous malformations (AVMs). The clinical sequelae of HHT2 include cutaneous and gastrointestinal bleeding, stroke and high output heart failure (HOHF). ALK-1 is a type I receptor for the TGF-β superfamily of ligands including TGFβ1 and bone morphogenetic proteins (BMP). Homozygous loss of ALK-1 causes embryonically lethality due to aberrant angiogenesis. For this reason, conditional knockout lines have been developed to study the post-natal effects of ALK-1 deficiency [1,2]. Conditional deletion of ALK-1 from the endothelial cell, but not vascular smooth muscle or pericyte, results in AVM formation, thereby implicating disrupted ALK-1 signaling in endothelial cells as a potential pathogenic mechanism for HHT2.

No studies have reported the effect of global ALK-1 deletion on cardiac hemodynamics and molecular indices of cardiac remodeling. The R26-Cre ER ALK-1 conditional knockout mouse (cKO) harbors the ROSA26-CreER knock-in allele whereby a single dose of intraperitoneal tamoxifen triggers ubiquitous Cre recombinase mediated excision of ALK-1. Prior studies of ALK-1 cKO mice have reported only gross cardiac hypertrophy and dilation [3,4]. In this study, we explored the central hypothesis that global ALK-1 deletion impairs cardiac function and promotes adverse cardiac remodeling.

Methods

Animal procedures

Animals were treated in compliance with the *Guide for the Care and Use of Laboratory Animals* (National Academy of Science) and all animal procedures were approved by the Tufts Medical Center Institutional Animal Care and Use Committee. The ROSA26-CreER knock-in mouse line ($R26^{+/CreER}$) ubiquitously expresses CreER and was crossed to mice harboring two floxed Alk1 alleles ($Alk1^{2loxP/2loxP}$). $R26^{+/CreER}$ $Alk1^{2loxP/2loxP}$ mice are a model of conditional ALK-1 deletion (cKO) whereby a single dose of tamoxifen activates global Cre mediated excision of Alk1 as described previously [4]. 4-Hydroxytamoxifen was dissolved in ethanol at a concentration of 10 mg/ml and stored at −80° prior to use. Tamoxifen aliquots were emulsified at a 1:5 ratio in sunflower seed oil and ethanol was evaporated in a speed-vac prior to intraperitoneal injection. cKO male mice aged 12–14 weeks of age were administered a single dose of intraperitoneal tamoxifen at a dose of 2.5

mg/25 g body weight (cKO-TAM). Age and gender matched cKO mice given vehicle (cKO-CON) or C57Bl/6 wild-type mice given tamoxifen (WT-TAM) served as controls. Mice were monitored daily and animals that exhibited severely reduced movement or loss of more than 25% of initial body weight were euthanized. To detect blood in the stool, samples were tested with the Hemoccult II SENSA card as per the manufacturer's instructions (Beckman Coulter).

Echocardiography

Transthoracic echocardiography was performed under light sedation with isoflurane administered via nose cone with core body temperature maintained at 37.0±0.2°C. A HDI5000 Machine (ATL Inc.) and a 10 MHz linear array transducer were used to record short axis M-mode tracings. Left ventricular end-diastolic and end-systolic diameters were measured and averaged across three cardiac cycles. Fractional shortening was calculated using the equation FS=(End diastolic diameter-End systolic diameter)/End diastolic diameter..

Pressure-Volume Loop Analysis

Terminal hemodynamic evaluation was performed in all animals. Mice were anesthetized with 2.0% isoflurane administered via a non-invasive nose cone. Body temperature was monitored by a rectal thermistor probe and maintained at 37.5°C with heating pads and a cycling heat lamp. In the supine position, the right common carotid artery was surgically isolated. A silk tie was placed at the distal end of the vessel and an overhand loop with 7-0 nylon was placed at the proximal end of the vessel. A Millar PVR-1045 conductance catheter (Millar Instruments) was introduced after calibration using the cuvette method with freshly heparizined warm blood as previously described [5]. For LV cannulation, a micro vascular clip was placed proximal to the overhand loop then a transverse arteriotomy was performed with iris scissors and the conductance catheter was advanced to the clip. The proximal nylon was then tightened around the vessel and the catheter. After removal of the surgical clip, the catheter was advanced past the aortic valve into the LV. Pressure-volume loop acquisition and analysis was performed using IOX software (EMKA). After data acquisition, the mouse was euthanized by direct injection of 0.3 ml 1 N KCL into the left ventricle. The heart was removed and processed for further analysis.

Real time Quantitative Polymerase Chain Reaction (RT-PCR)

Total RNA was extracted from the left ventricle (LV) with Trizol (Life Technologies) and converted to cDNA with a High Capacity cDNA Reverse Transcription Kit (Applied Biosystems). PCR was performed in triplicate using 40 cycles at 94°C for 15 seconds, 60°C for 30 seconds and 72°C for 30 seconds with an ABI Prism 7900 Sequence Detection System. Primers for 18S ribosomal RNA, Endoglin, TGF-β1, β-MHC, SERCA, Type I collagen and plasminogen activator inhibitor I (PAI-I) were used as described previously [6–8]. Primer sequences for activin like kinase-1 (ALK-1) were 5′-TGA CTT TCT GCA GAG GCA GA and 3′-CGA CTC AAA GCA GTC TGT GC, for activin like kinase 5 (ALK-5) were 5- ATC CAT CAC TAG ATC GCC CT and 3′-CGA TGG ATC AGA AGG TAC AAG A, for BMP-7 were 5′-ACC CTT CAT GGT GGC CTT CT and 3′-CCT CAG GGC CTC TTG GTT CT, for BMP-9 were 5′-TGT ACA ACA GGT ACA CGT CCG and 3′-TGA

ATG TCC TGG GAC ACC AG, for brain natriuretic peptide (BNP) were 5′-GTG AGG CCT TGG TCC TTC AA and 3′-CAC CGC TGG GAG GTC ACT and for connective tissue growth factor (CTGF) were 5′-AGC CTC AAA CTC CAA ACA CC and 3′-CAA CAG GGA TTT GAC CAC.

Histologic Quantification of Cardiac Hypertrophy and Fibrosis

Horizontal short-axis cut hearts were fixed in 10% formalin. Collagen abundance in the left ventricle was quantified by picrosirius red staining as a percentage of the total LV area. Cardiomyocyte cross-sectional area was quantified by identifying centrally nucleated and round cardiomyocytes on hematoxylin and eosin stained sections. Individual myocytes were traced after image acquisition and measured using ImageJ software (available online at http://imagej.nih.gov/ij/).

Statistics

All statistical analyses were performed using Graph Pad Prism v6 (Graph Pad Software, Inc.). Comparison between two experimental groups was performed with the unpaired student's T test and for three groups with a one-way ANOVA. α values less than 0.05 were accepted as statistically significant.

Results

cKO-TAM mice demonstrated reduced 14 day survival compared to cKO-CON and WT-TAM mice (13% vs 100%) (Figure 1C). At the time of harvest on day 14, cKO-TAM mice exhibited colonic hemorrhage, pale paws, melena and guiaic positive stools, indicative of internal hemorrhage and anemia (Figure 1A–B) [3,4]. After 14 days, total body weight was reduced and both LV and lung mass were increased in cKO-TAM mice, not WT-TAM or cKO-CON mice (Table 1). Beginning 7 days after tamoxifen treatment, cKO-TAM mice displayed a progressive reduction of left ventricular (LV) fractional shortening and increased LV end-diastolic volume (LV-EDV) (Figure 1C and Figure 2A–B). No change in LV-FS or LV-EDV was observed in cKO-CON mice. Compared to cKO-CON mice, surviving cKO-TAM mice exhibited reduced LV systolic pressure, increased end-diastolic pressure, and an increase in both stroke volume and cardiac output with no change in heart rate (Table 2, Figure 2A). Arterial elastance was lower in cKO-TAM mice compared to cKO-CON. These findings suggest that despite developing heart failure, global deletion of ALK-1 was associated with increased cardiac output and reduced arterial elastance.

To characterize the effects of global ALK-1 deletion on cardiac remodeling, we first identified reduced mRNA levels of ALK-1 in cKO-TAM, not cKO-CON mice (Figure 3A). We confirmed lower levels of ALK-1 mRNA levels in the liver (1.06 ± 0.32 vs. 0.23 ± 0.13) and lung (0.98 ± 0.27 vs. 0.22 ± 0.09, cKO-CON vs. cKO-TAM, fold change, $p<0.01$). LV mRNA levels of other TGF-β family receptors implicated in cardiac remodeling (ALK-5, Endoglin) were unchanged in cKO-TAM compared to cKO-CON mice (Figure 3B–C). LV mRNA levels of ligands associated with ALK-1 signaling including TGF-β1, BMP-7 and BMP-9 were similar among all groups (Figure 3D–F). Next, we examined parameters of cardiac hypertrophy and identified increased cardiomyocyte area (Figure 4A–B) and a ~2

fold increase in BNP levels among cKO-TAM mice, not CKO-CON or WT TAM mice (Figure 4C). Levels of markers associated with maladaptive hypertrophy including beta-myosin heavy chain (β-MHC) and of sarcoplasmic endoplasmic reticulum ATPase (SERCA) were unchanged (Figure 4D–E) among all groups. We then quantified indices of cardiac fibrosis and observed increased no change in collagen abundance or mRNA levels of Type I collagen, CTGF, or PAI-1 among all groups. (Figure 5A–E).

Discussion

The central finding of this report is that global ALK-1 deletion leads to early mortality and high output heart failure due to the development of AVMs and anemia due to internal hemorrhage. We specifically introduce for the first time hemodynamic data in conditional ALK-1 knockout mice showing reduced LV systolic function and high LV filling pressures, but increased stroke volume and cardiac output in the presence of low arterial elastance. The observed reduction in arterial elastance may be due to anemia and the presence of systemic shunting via AVMs. Consistent with these hemodynamic data, we further show that despite developing systolic heart failure, canonical pathways associated with maladaptive cardiac remodeling are not activated. Further evidence supporting the development of high output heart failure, hearts from conditional ALK-1 knockout mice showed cardiac hypertrophy without fibrosis.

These findings have several major implications. First, heart failure among patients with HHT-2 remains poorly understood. It is not known if heart failure among these patients is characterized by adaptive remodeling characterized by cardiac hypertrophy without fibrosis or maladapative remodeling characterized by hypertrophy, fibrosis and induction of fetal gene expression. A maladaptive pattern of cardiac remodeling with excess fibrosis has been associated with adverse clinical outcomes in patients with heart failure [9–11]. Using a mouse model with typical phenotypic features of HHT2, we now show that congestive heart failure is due to high output heart failure with evidence of adaptive as opposed to maladaptive remodeling. The distinction between adaptive and maladaptive remodeling is critical as interventions to correct the high output state in patients with HHT-2, such as correction of shunting and anemia, would be expected to reverse remodeling if the changes are adaptive. Second, ALK-1 inhibitors have been recently developed for cancer therapeutics. Since chemotherapy is often associated with maladaptive remodeling, our data suggest that high output heart failure must be ruled out in patients treated with ALK-1 inhibitors who develop systolic heart failure. Finally, these data suggest that suggest that early signs of systolic heart failure can develop shortly after the onset of clinically relevant AVMs. Routine screening of patients with phenotypic features of HHT-2 for systolic dysfunction may allow for early intervention to prevent the onset of congestive heart failure.

HOHF is a frequent and morbid presentation of patients with HHT2. The formation of systemic AVMs, most often in the liver, lead to a left to right shunt and increased cardiac output through a reduction in arterial load [12]. Liver involvement is observed in a majority of patients with HHT2 and HOHF is the most common complication with an increased mortality risk [13]. However only 8% of patients with liver AVMs develop symptoms and new onset HOHF is often the initial symptomatic manifestation of previously undiagnosed

HHT2 [13–16]. It has been observed that most patients with liver involvement have evidence of increased cardiac output and/or elevated left ventricular filling pressures, suggesting an asymptomatic high output state may precede the development of symptomatic heart failure [13,17,18]. Early recognition of HOHF is clinically relevant as conventional medical therapy for heart failure, anti-VEGF antibody treatment or orthotopic liver transplantation, have been shown to improve outcomes in selected patients with HHT and HOHF [13,14,19].

While HOHF is a common and serious complication of HHT, cardiac function and remodeling in models of HHT has not been reported. HOHF has been examined in prior literature most frequently through surgical induction of an aorta-caval shunt [16,20,21]. Mortality in this model occurs mainly in the peri-operative period and in animals with large shunt fractions; thereafter the resultant HOHF does not significantly impact survival through four weeks [16,20,21]. Early mortality (before 14 days) was observed in conditional ALK-1 knockout mice, suggesting uncontrolled hemorrhage and anemia in the context of HOHF was not well tolerated. In aorta-caval shunt models, an induction of BNP expression, but not markers of pathological remodeling, including upregulation of β-MHC and downregulation of SERCA, has been observed [21–23]. We observed a small induction of BNP expression without activation of the maladaptive remodeling program. With the exception of the expected reduction in ALK-1 expression, other ligands and receptors of the TGF-β family were not perturbed in the LV. Further, while cardiomyocyte hypertrophy was observed, upregulation of fibrotic markers and fibrotic deposition was not seen in the LV. Taken together, our data indicate that the remodeling observed in HOHF due to HHT and surgical shunt models is adaptive and agree with the clinical observation that therapeutic resolution of shunting results in improved cardiac function and HF symptoms in most patients [14,19,24].

In conclusion, this is the first report to study the effect of global ALK-1 deletion on cardiac hemodynamic and indices of cardiac remodeling. Our findings suggest that the cKO-ALK1 mouse represents a rarely observed transgenic model to study high output heart failure. Future studies are required to study the reversibility of HOHF in this model and to better understand whether ALK-1 plays a role in cardiac remodeling independent of systemic AVMs.

References

1. Tual-Chalot S, Oh SP, Arthur HM. Mouse models of hereditary hemorrhagic telangiectasia: recent advances and future challenges. Front Genet. 2015; 6:25. [PubMed: 25741358]
2. Oh SP, Seki T, Goss KA, Imamura T, Yi Y, Donahoe PK, Li L, Miyazono K, ten Dijke P, Kim S, Li E. Activin receptor-like kinase 1 modulates transforming growth factor-beta 1 signaling in the regulation of angiogenesis. Proc Natl Acad Sci U S A. 2000; 97:2626–2631. [PubMed: 10716993]
3. Han C, Choe SW, Kim YH, Acharya AP, Keselowsky BG, Sorg BS, Lee YJ, Oh SP. VEGF neutralization can prevent and normalize arteriovenous malformations in an animal model for hereditary hemorrhagic telangiectasia 2. Angiogenesis. 2014; 17:823–830. [PubMed: 24957885]
4. Park SO, Wankhede M, Lee YJ, Choi EJ, Fliess N, Choe SW, Oh SH, Walter G, Raizada MK, Sorg BS, Oh SP. Real-time imaging of de novo arteriovenous malformation in a mouse model of hereditary hemorrhagic telangiectasia. J Clin Invest. 2009; 119:3487–3496. [PubMed: 19805914]

5. Rockman HA, Ono S, Ross RS, Jones LR, Karimi M, Bhargava V, Ross J Jr, Chien KR. Molecular and physiological alterations in murine ventricular dysfunction. Proc Natl Acad Sci U S A. 1994; 91:2694–2698. [PubMed: 8146176]

6. Kapur NK, Paruchuri V, Aronovitz MJ, Qiao X, Mackey EE, Daly GH, Ughreja K, Levine J, Blanton R, Hill NS, Karas RH. Biventricular remodeling in murine models of right ventricular pressure overload. PLoS One. 2013; 8:e70802. [PubMed: 23936252]

7. Kapur NK, Qiao X, Paruchuri V, Mackey EE, Daly GH, Ughreja K, Morine KJ, Levine J, Aronovitz MJ, Hill NS, Jaffe IZ, Letarte M, Karas RH. Reducing endoglin activity limits calcineurin and TRPC-6 expression and improves survival in a mouse model of right ventricular pressure overload. J Am Heart Assoc. 2014; 3:e000965. [PubMed: 25015075]

8. Kapur NK, Wilson S, Yunis AA, Qiao X, Mackey E, Paruchuri V, Baker C, Aronovitz MJ, Karumanchi SA, Letarte M, Kass DA, Mendelsohn ME, Karas RH. Reduced endoglin activity limits cardiac fibrosis and improves survival in heart failure. Circulation. 2012; 125:2728–2738. [PubMed: 22592898]

9. Fukui M, Goda A, Komamura K, Nakabo A, Masaki M, Yoshida C, Hirotani S, Lee-Kawabata M, Tsujino T, Mano T, Masuyama T. Changes in collagen metabolism account for ventricular functional recovery following beta-blocker therapy in patients with chronic heart failure. Heart Vessels. 2016; 31:173–182. [PubMed: 25351137]

10. Harada M, Hojo M, Kamiya K, Kadomatsu K, Murohara T, Kodama I, Horiba M. Exogenous midkine administration prevents cardiac remodeling in pacing-induced congestive heart failure of rabbits. Heart Vessels. 2016; 31:96–104. [PubMed: 25155308]

11. Ikeda Y, Inomata T, Fujita T, Iida Y, Nabeta T, Ishii S, Maekawa E, Yanagisawa T, Mizutani T, Naruke T, Koitabashi T, Takeuchi I, Ako J. Cardiac fibrosis detected by magnetic resonance imaging on predicting time course diversity of left ventricular reverse remodeling in patients with idiopathic dilated cardiomyopathy. Heart Vessels. 2016; 31:1817–1825. [PubMed: 26843195]

12. Garcia-Tsao G, Korzenik JR, Young L, Henderson KJ, Jain D, Byrd B, Pollak JS, White RI Jr. Liver disease in patients with hereditary hemorrhagic telangiectasia. N Engl J Med. 2000; 343:931–936. [PubMed: 11006369]

13. Buscarini E, Leandro G, Conte D, Danesino C, Daina E, Manfredi G, Lupinacci G, Brambilla G, Menozzi F, De Grazia F, Gazzaniga P, Inama G, Bonardi R, Blotta P, Forner P, Olivieri C, Perna A, Grosso M, Pongiglione G, Boccardi E, Pagella F, Rossi G, Zambelli A. Natural history and outcome of hepatic vascular malformations in a large cohort of patients with hereditary hemorrhagic teleangiectasia. Dig Dis Sci. 2011; 56:2166–2178. [PubMed: 21290179]

14. Dupuis-Girod S, Ginon I, Saurin JC, Marion D, Guillot E, Decullier E, Roux A, Carette MF, Gilbert-Dussardier B, Hatron PY, Lacombe P, Lorcerie B, Rivière S, Corre R, Giraud S, Bailly S, Paintaud G, Ternant D, Valette PJ, Plauchu H, Faure F. Bevacizumab in patients with hereditary hemorrhagic telangiectasia and severe hepatic vascular malformations and high cardiac output. JAMA. 2012; 307:948–955. [PubMed: 22396517]

15. Faughnan ME, Palda VA, Garcia-Tsao G, Geisthoff UW, McDonald J, Proctor DD, Spears J, Brown DH, Buscarini E, Chesnutt MS, Cottin V, Ganguly A, Gossage JR, Guttmacher AE, Hyland RH, Kennedy SJ, Korzenik J, Mager JJ, Ozanne AP, Piccirillo JF, Picus D, Plauchu H, Porteous ME, Pyeritz RE, Ross DA, Sabba C, Swanson K, Terry P, Wallace MC, Westermann CJ, White RI, Young LH, Zarrabeitia R. HHT Foundation International - Guidelines Working Group. International guidelines for the diagnosis and management of hereditary haemorrhagic telangiectasia. J Med Genet. 2011; 48:73–87. [PubMed: 19553198]

16. Garcia-Tsao G. Liver involvement in hereditary hemorrhagic telangiectasia (HHT). J Hepatol. 2007; 46:499–507. [PubMed: 17239481]

17. Gincul R, Lesca G, Gelas-Dore B, Rollin N, Barthelet M, Dupuis-Girod S, Pilleul F, Giraud S, Plauchu H, Saurin JC. Evaluation of previously nonscreened hereditary hemorrhagic telangiectasia patients shows frequent liver involvement and early cardiac consequences. Hepatology. 2008; 48:1570–1576. [PubMed: 18972447]

18. Ginon I, Decullier E, Finet G, Cordier JF, Marion D, Saurin JC, Dupuis-Girod S. Hereditary hemorrhagic telangiectasia, liver vascular malformations and cardiac consequences. Eur J Intern Med. 2013; 24:e35–39. [PubMed: 23312966]

19. Lerut J, Orlando G, Adam R, Sabbà C, Pfitzmann R, Klempnauer J, Belghiti J, Pirenne J, Thevenot T, Hillert C, Brown CM, Gonze D, Karam V, Boillot O. European Liver Transplant Association. Liver transplantation for hereditary hemorrhagic telangiectasia: Report of the European liver transplant registry. Ann Surg. 2006; 244:854–862. [PubMed: 17122610]

20. Karram T, Hoffman A, Bishara B, Brodsky S, Golomb E, Winaver J, Abassi Z. Induction of cardiac hypertrophy by a controlled reproducible sutureless aortocaval shunt in the mouse. J Invest Surg. 2005; 18:325–334. [PubMed: 16319054]

21. Scheuermann-Freestone M1, Freestone NS, Langenickel T, Höhnel K, Dietz R, Willenbrock R. A new model of congestive heart failure in the mouse due to chronic volume overload. Eur J Heart Fail. 2001; 3:535–543. [PubMed: 11595601]

22. Braun MU, LaRosée P, Simonis G, Borst MM, Strasser RH. Regulation of protein kinase C isozymes in volume overload cardiac hypertrophy. Mol Cell Biochem. 2004; 262:135–143. [PubMed: 15532718]

23. Calderone A, Takahashi N, Izzo NJ Jr, Thaik CM, Colucci WS. Pressure- and volume-induced left ventricular hypertrophies are associated with distinct myocyte phenotypes and differential induction of peptide growth factor mRNAs. Circulation. 1995; 92:2385–2390. [PubMed: 7586335]

24. Boillot O, Bianco F, Viale JP, Mion F, Mechet I, Gille D, Delaye J, Paliard P, Plauchu H. Liver transplantation resolves the hyperdynamic circulation in hereditary hemorrhagic telangiectasia with hepatic involvement. Gastroenterology. 1999; 116:187–192. [PubMed: 9869617]

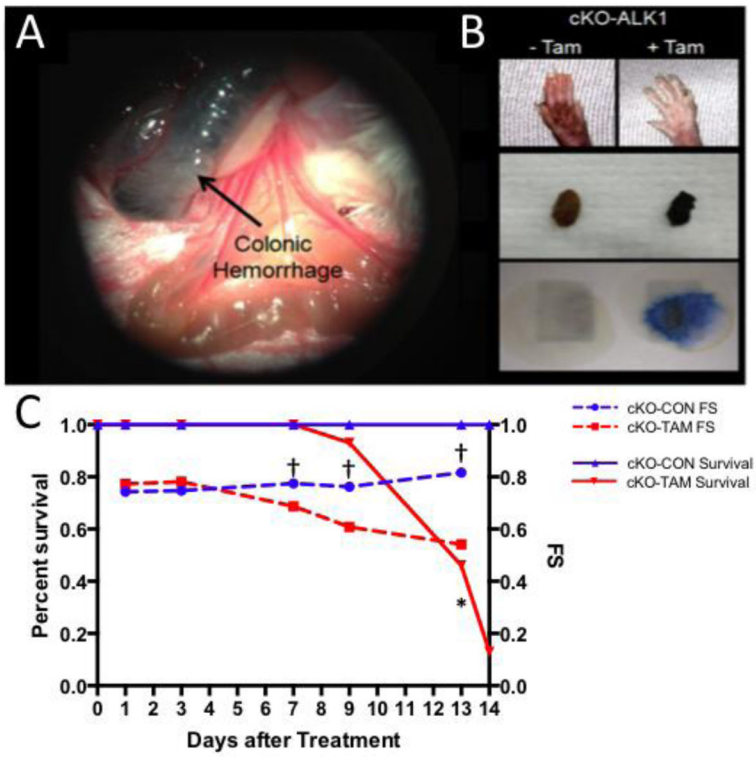

Fig 1. Phenotype of total body ALK-1 depletion

ALK-1 cKO mice treated with tamoxifen developed (A) colonic hemorrhage observed 13 days after tamoxifen treatment, (B) pale paws observed 10 days after Tamoxifen treatment, melena, and guaiac positive stool. (C) Compared to vehicle treated controls (cKO-CON), cKO-TAM mice demonstrated early mortality and a corresponding reduction in LV fractional shortening. *, $p<0.05$, vs. cKO CON Survival and †, $p<0.05$, vs. cKO CON FS.

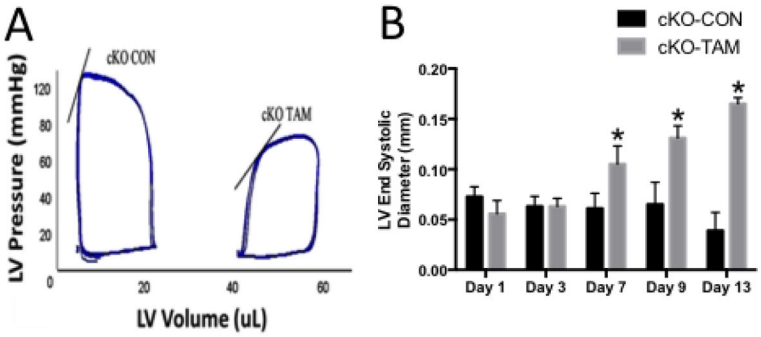

Fig 2. ALK-1 depletion promotes high output heart failure

(A) Representative pressure volume loops demonstrate lower LV systolic pressure and increased LV end-systolic and end-diastolic volumes in cKO-TAM compared to cKO-CON mice after 14 days after tamoxifen treatment. Solid line indicates the end systolic pressure volume relationship. Echocardiography showed (B) increased LV end-systolic diameter beginning 7 days after treatment in cKO-TAM, not cKO-CON mice. *, $p<0.05$ vs. cKO-CON at the same time point; n=5/group.

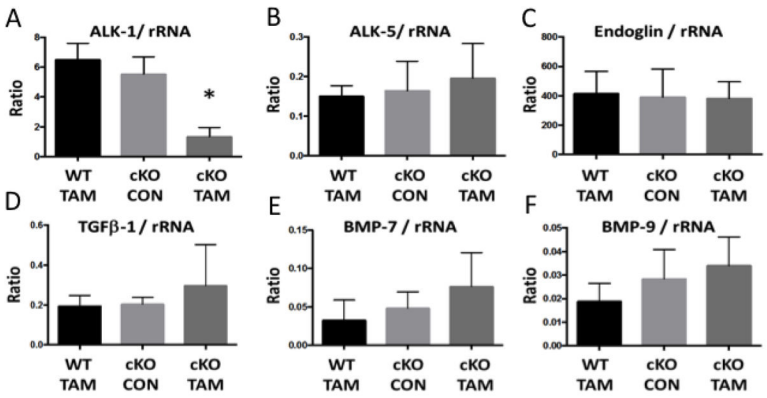

Fig 3. Left ventricular expression of TGF-β family receptors and ligands

Compared to cKO-CON, cKO-TAM mice demonstrated (A) reduced mRNA levels of ALK-1 in the LV at 14 days after tamoxifen treatment. No change in (B–E) ALK-5, Endoglin, TGF-β1, BMP-7 or BMP-9 were observed in the cKO-TAM LV. *, $p<0.05$ vs. WT-TAM or cKO-CON; n=5/group.

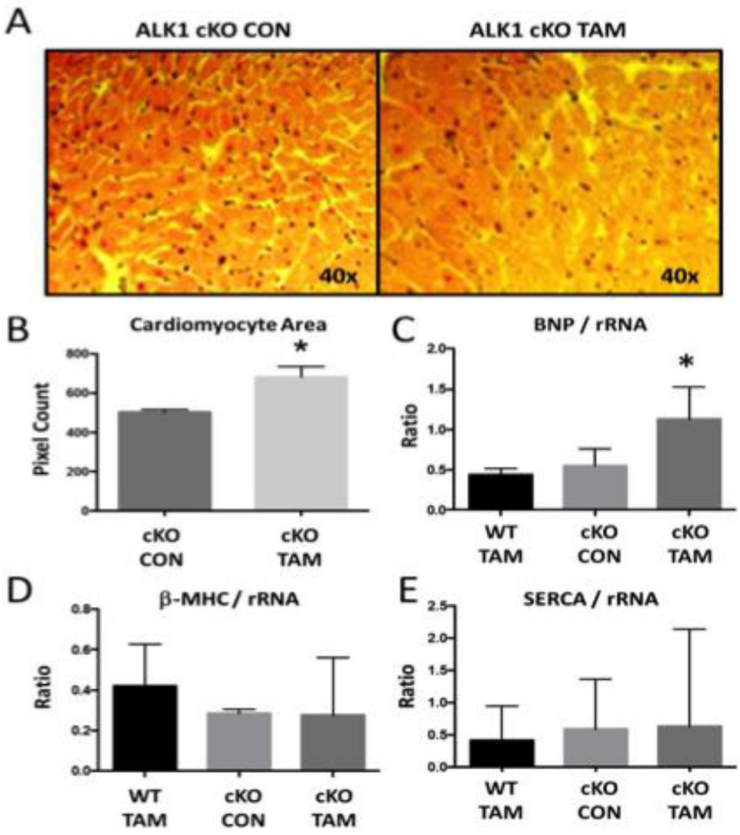

Fig 4. ALK-1 depletion is associated with cardiomyocyte hypertrophy

Compared to cKO-CON, cKO-TAM mice demonstrated (A–B) increased cardiomyocyte cross-sectional area, (C) increased levels of BNP mRNA in the LV, and no change in LV levels of (D) β-MHC or (E) SERCA mRNA at 14 days after tamoxifen treatment. *, $p<0.05$ vs WT-TAM or cKO-CON; n=5/group.

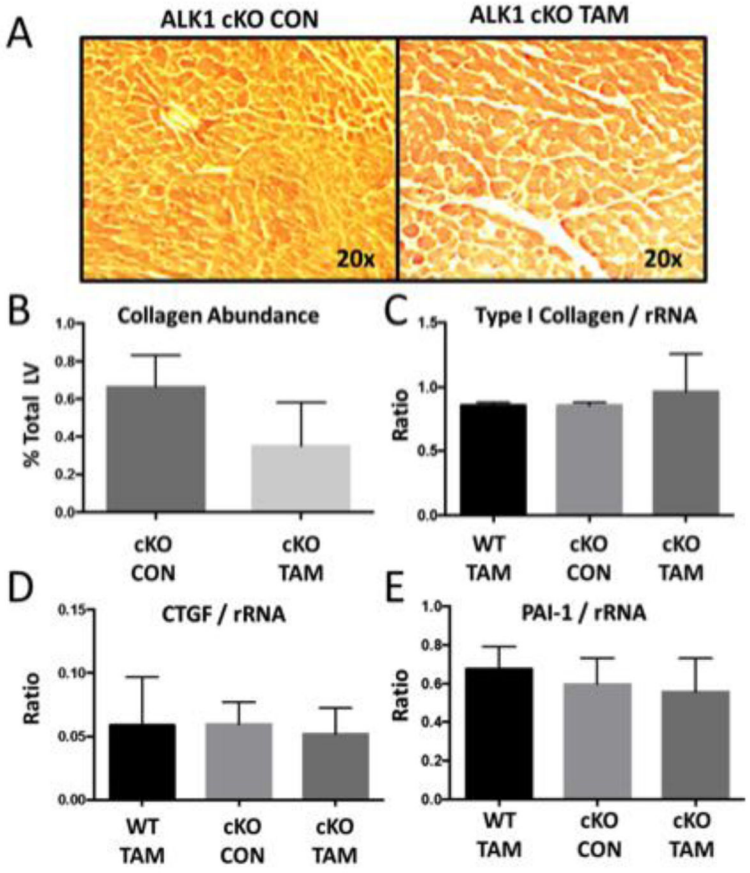

Fig 5. ALK-1 depletion is not associated with cardiac fibrosis

Compared to cKO-CON, cKO-TAM mice demonstrated no change in (A–B) collagen abundance with picrosirius red staining or (C–E) LV levels of Type I collagen, connective tissue growth factor (CTGF), or plasminogen activator inhibitor-1 (PAI-1) mRNA at 14 days after tamoxifen treatment.

Table 1

Characteristics of wild-type mice treated with tamoxifen (WT TAM), ALK1 cKO mice treated with vehicle (cKO CON), or ALK1 cKO mice treated with tamoxifen (cKO TAM) for fourteen days.

	WT TAM (n=5)	cKO CON (n=5)	cKO TAM (n=7)
Total body weight (g)	24.9 ± 2.8	27.7 ± 7.9	21.3 ± 2.4 *
LV mass (mg)	77.1 ± 3.8	71.1 ± 4.7	96.8 ± 9.0 *
Lung mass (mg)	168.0 ± 11.3	151.0 ± 24.3	255.7 ± 98.8 *
Tibia length (mm)	17.8 ± 0.5	17.7 ± 0.5	17.5 ± 0.4
LV/TBW (mg/g)	3.1 ± 0.2	2.7 ± 0.6	4.6 ± 0.4 *
LV/TL (mg/mm)	4.3 ± 0.1	4.0 ± 0.1	5.5 ± 0.4 *

Table 2

Left ventricular hemodynamics of cKO-CON and cKO-TAM mice at 14 days after tamoxifen treatment.

LV Hemodynamics	cKO-CON (n=5)	cKO-TAM (n=7)
Peak systolic pressure (mmHg)	95±9	72±4 *
End diastolic pressure (mmHg)	5.2±3	12.5±4.8 *
Max dP/dt (mmHg/sec)	10202±1227	6271±2262 *
Cardiac output (uL/min)	6742±1457	8818±1052 *
Effective arterial elastance (mmHg/mL)	7.6±1.7	3.9±0.6 *
Heart rate (beats per minute)	528±27	497±12